Biophysical Chemistry 11 (1980) 309–316

LOW FREQUENCY DIELECTRIC RELAXATION AND LIGHT SCATTERING UNDER AC ELECTRIC FIELD OF DNA SOLUTIONS

Masanori SAKAMOTO*, Takashi FUJIKADO**, Reinosuke HAYAKAWA and Yasaku WADA
Department of Applied Physics, Faculty of Engineering, University of Tokyo, Bunkyo-ku, Tokyo 113, Japan

Low frequency dielectric relaxation of aqueous DNA was measured in a frequency range from 0.1 Hz to 30 kHz. Agreement was found between dielectric relaxation time and rotational one estimated from reduced viscosity for dilute solutions of DNA. The low frequency relaxation is thus ascribed to rotation of the major axis of DNA chains elongated by electrostatic repulsion between charges on the chain. A quasi-permanent dipole moment of DNA estimated from the dielectric increment is well explained by the fluctuation of dissociation of DNA. The above conclusion was confirmed for DNA samples of various molecular weights and for solutions in water ethanol mixtures. Effects of binding of salts and dyes are also interpreted in terms of the same mechanism. Light scattering of aqueous DNA under a.c. electric field supports the above conclusion.

1. Introduction

Low frequency dielectric relaxation of DNA and other polyelectrolytes in aqueous dilute solution has been studied for many years for the purpose of elucidating the dynamic behavior of polyions and counterions [1–11].

Owing to limitation of the measuring frequency range, however, the overall nature of the relaxation had not been revealed until recently [12–15]. Our new technique, the simultaneous two-frequency measurement with a four-electrode cell, made it possible to avoid the effects of high d.c. conductivity and electrode polarization and measure the complex dielectric constant of DNA solutions in a wide frequency range from 0.1 Hz to 30 kHz. As a result, the low frequency relaxation of DNA has been clarified for various conditions of sample solutions with varying molecular weight M_r of DNA [13], solvent composition [14], DNA concentration C_p [14], added salt species and concentration [15], and dye species and concentration [15].

The results indicate that the low frequency dielectric relaxation of DNA is ascribed to rotation of DNA molecules with a quasi-permanent dipole due to fluctuation in dissociation of DNA [12]. Here the fluctuation is assumed to be slower than the rotation and thus induces a dipole moment with a life-time longer than the rotational relaxation time.

In addition to the dielectric spectroscopy, we have developed the following new techniques and improvements of conventional techniques for the purpose of studying the dynamic behavior of DNA and other polyelectrolytes:

(1) Light scattering under an a.c. electric field [16].

(2) Birefringence under an a.c. electric field [17].

(3) Birefringence under a sinusoidally varying shear flow [18].

(4) Viscoelasticity [19].

(5) Computer simulation of Brownian motion of model polyelectrolyte [20].

Results obtained by these techniques support also the conclusion of the dielectric spectrometry: DNA and other polyelectrolytes such as poly(acrylic acid) possess an elongated form due to electrostatic repulsion between charges on the chain and the reorientational motion of the major axis of the molecule causes the low frequency relaxation.

This paper summarizes our recent results on low frequency dielectric relaxation [12–15] and electric field light scattering [16] of DNA.

* Present address: Research & Development Center, Tokyo Shibaura Electric Co., Ltd., Saiwai-ku, Kawasaki 210, Japan.
** Present address: 2-165 Ohtamachi, Minato-ku, Yokohama 233, Japan.

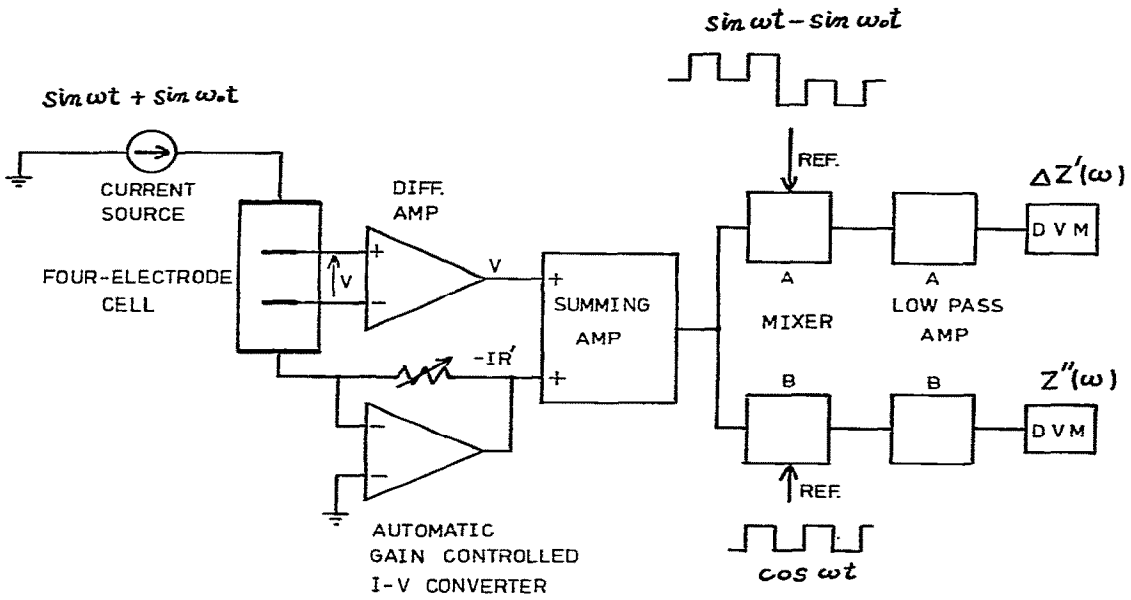

Fig. 1. Block diagram of the apparatus for simultaneous two-frequency measurement of complex dielectric constant. $Z^* = Z' + iZ''$ denotes complex impedance of solution.

2. Experimental

Our new technique for measuring complex dielectric constant $\epsilon^* = \epsilon' - i\epsilon''$ of a highly conductive material consists in the following points [21,22]:

(1) A four-electrode cell to avoid the effect of electrode polarization.

(2) An automatic rough bridge balance for eliminating roughly the effect of d.c. conductivity to avoid saturation of the input amplifier.

(3) Simultaneous two-frequency measurement for completely eliminating the effect of d.c. conductivity.

(4) Comparative measurement of solution and solvent for avoiding the effect of leakage flux, etc.

Fig. 1 shows the block diagram of the apparatus. We apply to the current electrodes the sum of sinusoidal currents at two frequencies, $\sin \omega t + \sin \omega_0 t$, and detect the induced voltage across the potential electrodes. The voltage is demodulated by a reference wave $\sin \omega t - \sin \omega_0 t$ and we get directly the difference, $\Delta[\omega\epsilon''(\omega)] = \omega\epsilon''(\omega) - \omega_0\epsilon''(\omega_0)$, in which the d.c. conductivity σ is completely eliminated. ω_0 is fixed at a constant value and ω is varied in the measuring fre-

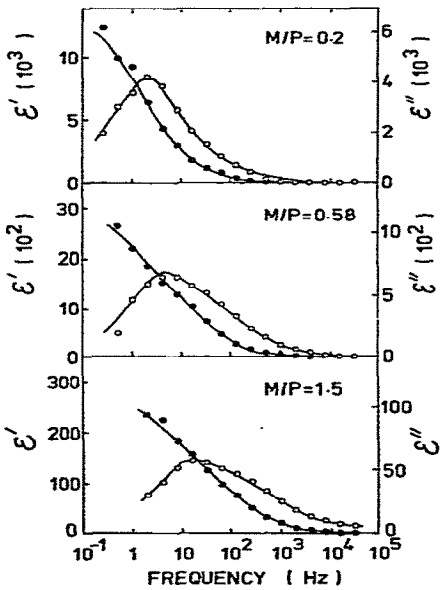

Fig. 2. Real (•) and imaginary (○) parts of complex dielectric constant of aqueous DNA ($M_I = 4 \times 10^6$, $C_p = 0.01\%$) at three concentrations of $AgNO_3$ (M/P denoting molarity ratio of $AgNO_3$ and phosphate residue).

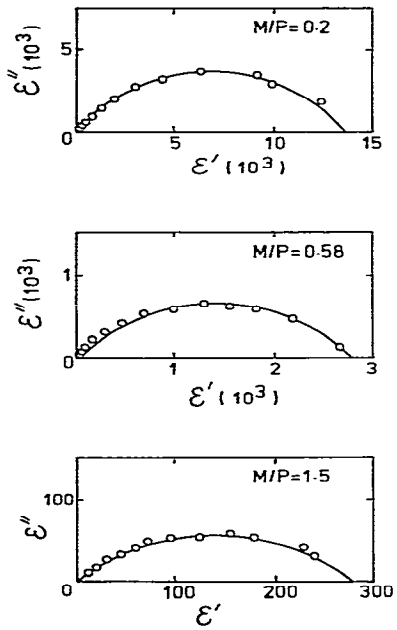

Fig. 3. Cole-Cole plots of the data in fig. 2.

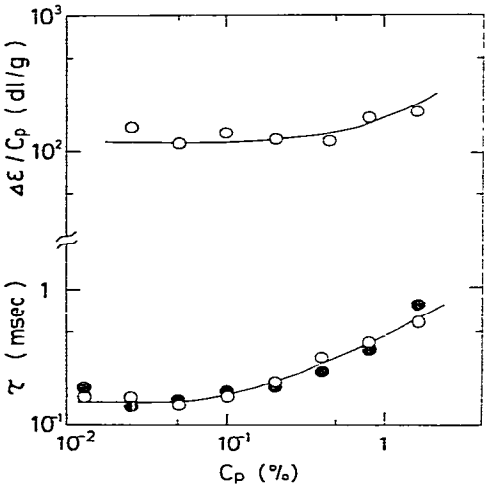

Fig. 4. Specific increment $\Delta\epsilon/C_p$(○) and dielectric relaxation time (○) of aqueous DNA ($M_r = 5 \times 10^5$, 1mM NaCl) plotted against DNA concentration. Closed circles represent rotational relaxation time.

quency range. For the real part ϵ' in which σ is not involved, we demodulate the voltage simply by $\cos \omega t$ and we get $\omega\epsilon'(\omega)$. By use of this technique, we could extend the frequency range from 0.1 Hz to 30 kHz for a dilute solution of DNA ($C_p = 0.01\%$ to 0.1% corresponding to $M_r = 4 \times 10^6$ to 4×10^5) in 1 mM NaCl.

The dielectric increment $\Delta\epsilon = \epsilon'(0) - \epsilon'(\infty)$ is obtained from the Cole-Cole plot and the dielectric relaxation time τ_D from the equation $\tau_D = 1/(2\pi f_r)$ where f_r is the frequency at the peak of ϵ''. Figs. 2 and 3 represent examples of the data and their Cole-Cole plots, respectively.

In addition to the dielectric spectroscopy, we have developed a new apparatus for light scattering under an a.c. electric field [16]. Employment of chopping of the electric field (AM technique) increased greatly the S/N ratio for measuring the relative increment of scattered light intensity $r = \Delta I/I_0$ (ΔI: steady component of incremental light intensity due to electric field, I_0: scattered light intensity without electric field) as a function of frequency ω of electric field ranging from 10 Hz to 100 kHz. Furthermore, we introduced a frequency modulation technique (FM technique) in which a frequency-modulated a.c. electric field is applied to the solution and the frequency derivative of the dispersion curve is directly observed. The peak of the FM curve gives the relaxation frequency f_r.

The viscosity of the solution was measured with a Zimm-Crothers type viscometer with a very low shear rate. Measurements were made at 10°C for dielectric measurement and viscometry and at 25°C for light scattering measurement.

Original samples of DNA (sodium salt) were calf thymus DNA and salmon testis DNA purchased from Sigma Chem. Co. and P-L Biochemicals, Inc.. In some experiments, sonicated samples, fractionated ones and deproteinized ones were used. Procedures for these sample preparations were described elsewhere [13–15]. The molecular weight of the sample was determined from the intrinsic viscosity in 0.2M NaCl. C_p denotes the weight concentration of sodium salt of DNA through this paper.

3. Results and discussion

3.1. Effect of concentration

The dielectric relaxation was measured with varying DNA concentration. Fig. 4 represents results for DNA of $M_r = 5 \times 10^5$.

Table 1
Comparison of dielectric parameters for four pairs of DNA samples in 1 mM NaCl before and after deproteinization.

M_r (10^6)	Protein (wt.%)	C_p (wt.%)	τ_D (ms)	$\Delta\epsilon$	$\langle\mu^2\rangle^{1/2}$ (10^5D)	
					obs. (eq. 3)	calc. (eq. 4)
0.39	2.1	0.1	0.13	140	0.29	0.39
0.42	0.5	0.1	0.16	130	0.29	0.43
1.7	2.0	0.01	2.6	320	2.9	2.3
1.9	1.0	0.01	3.8	305	3.0	2.7
6.6	1.2	0.01	42	830	9.2	10
6.6	0.3	0.01	51	850	9.3	10
13	3.0	0.01	55	2700	23	20
13	1.3	0.01	51	2400	22	20

The C_p dependence of the specific increment $\Delta\epsilon/C_p$ and τ_D is rather weak below a critical concentration C_p^* but both $\Delta\epsilon/C_p$ and τ_D increase rapidly above C_p^*. Values of C_p^* were found to be 0.2% for DNA of $M_r = 5 \times 10^5$ in 1 mM NaCl (fig. 4) but 0.02% for $M_r = 2 \times 10^6$. These C_p^* values correspond to the concentration where $\langle S^2\rangle^{3/2}$ ($\langle S^2\rangle$ being the mean squared radius of gyration) is about one half of the volume of solution alloted to a DNA molecule.

Here $\langle S^2\rangle$ was calculated by the Kratky-Porod equation for a wormlike chain [23],

$$\langle S^2\rangle = qL/3 - q^2 + 2q^3/L - 2q^4/L^2 + (2q^4/L^2)\exp(-L/q)\,, \quad (1)$$

where L is the contour length and q the persistence length (q = 850 Å in 1 mM NaCl [14]). The conformation of DNA at low concentrations of added salt cannot be expressed by the wormlike chain model. In the present study, however, we estimated the effective persistence length so as to reproduce the observed reduced viscosity η_r of the solution by $\langle S^2\rangle$ in eq. (1), assuming the well-known relation, $\eta_r \propto \langle S^2\rangle^{3/2}/M_r$.

In the dilute range below C_p^*, τ_D was found to agree well with the rotational relaxation time τ (fig. 4) estimated from η_r of the same solution by the equation [14],

$$\tau = 0.85\eta_r\eta_s M_r/RT\,, \quad (2)$$

where η_s is the solvent viscosity and RT has the usual meaning. The data in the following subsections were obtained in the dilute range.

3.3. Origin of dipole moment

The agreement between τ_D and τ in the dilute range suggests that the low frequency dielectric relaxation arises from rotation of DNA molecules. In this case, the dielectric increment $\Delta\epsilon$ is related to the mean squared dipole moment $\langle\mu^2\rangle$ of the molecule as

$$\Delta\epsilon = 4\pi N\langle\mu^2\rangle/3kT\,, \quad (3)$$

where N is the number of molecules per unit volume and kT has the usual meaning.

The vectorial sum of bond dipole moments of DNA should be cancelled out in a double helix without defects. Protein contamination might be the origin of the dipole of DNA [9]. To check this possibility, we compared dielectric relaxations of DNA before and after deproteinization for four kinds of DNA samples. The results showed that protein contamination has only a minor effect to dielectric relaxation as listed in table 1.

Counterions around DNA are sometimes bound on DNA and sometimes free. If the change of counterions between bound and free states is slower than the rotation of DNA, the dipole due to this fluctuation is expected to function as a quasi-permanent dipole. The mean squared dipole moment due to this mechanism is given by [12,24]

$$\langle\mu^2\rangle = n\alpha(1-\alpha)e^2\langle S^2\rangle\,, \quad (4)$$

where n is the number of phosphate residues of a DNA molecule, α the effective degree of dissociation of DNA and e the elementary charge. α in aqueous NaCl was determined as 0.3 from the d.c. conductivity measurement

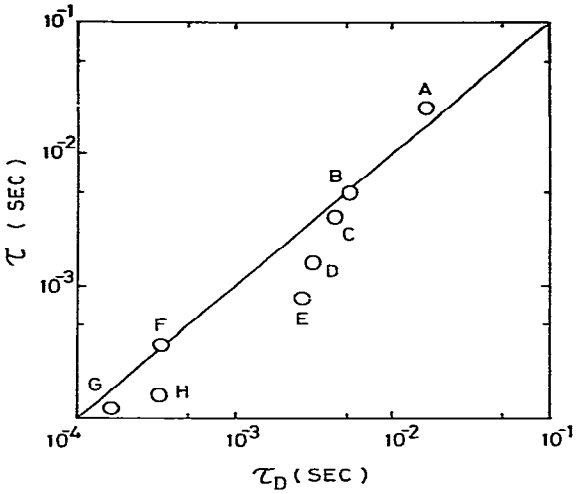

Fig. 5. Comparison of dielectric relaxation time τ_D and rotational one τ for DNA in 1 mM NaCl with various molecular weights: $M_r = 4\times10^6$, 2×10^6, 1.5×10^6, 1×10^6, 8×10^5, 6×10^5, 4×10^5 and 4×10^5 for A to H, respectively (reproduced from Sakamoto, Hayakawa and Wada [13]).

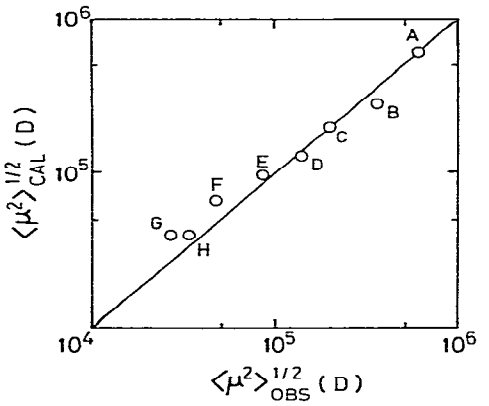

Fig. 6. Comparison of observed and calculated rms dipole moment of DNA. Samples are identified as in fig. 5.

of the solution [14] by the equation,

$$\sigma = e\,[\alpha n N u_{DNA} + (N_s + \alpha n N)u^+ + N_s u^-]\,, \qquad (5)$$

where u_{DNA} (3.4×10^{-4} cm^2/volt, s), u^+ and u^- are respectively mobilities of DNA, Na^+ and Cl^- and N_s the number of salt ions per unit volume.

In table 1, agreement between observed values of $\langle\mu^2\rangle$ and values calculated from eq. (4) is satisfactory. We conclude therefore that the origin of low frequency relaxation of DNA is the rotation of DNA molecule with a quasi-permanent dipole arising from fluctuation in the dissociation of DNA. Results in subsequent subsections conform well with this conclusion.

3.3. Effect of molecular weight

By use of sonicated fragments of DNA, we measured $\Delta\epsilon$ and τ_D for eight samples of DNA of different molecular weights. Results in figs. 5 and 6 show general agreements between τ_D and τ and between observed and calculated values of $\langle\mu^2\rangle^{1/2}$, respectively.

It was experimentally found that τ_D is proportional to M_r^2. Since the rotational relaxation time of a rigid rod is proportional to M_r^3 and that of a bead-spring model (model of a random coil) to $M_r^{1.5}$ [25], the present result indicates that DNA takes a conformation intermediate between the two extremes. $\langle\mu^2\rangle$ of DNA was found to be proportional to $M_r^{2.6}$ and thus $\langle S^2\rangle$ in eq. (4) should be proportional to $M_r^{1.6}$, being again an intermediate between rigid rod ($\langle S^2\rangle \propto M_r^2$) and random coil ($\langle S^2\rangle \propto M_r$).

3.4. Dielectric relaxation of DNA in water ethanol mixtures

Addition of ethanol to aqueous solution of DNA changes both dielectric constant ϵ_s and viscosity η_s of solvent. Since τ is proportional to $\eta_s\langle S^2\rangle^{3/2}$, the change in η_s directly affects τ. Furthermore, addition of ethanol decreases ϵ_s, which results in the increase of electrostatic repulsion between dissociated sites on DNA and at the same time the decrease of the effective degree of dissociation α. The latter effect is expressed, according to Manning [26], by the equation,

$$\alpha = kT\epsilon_s/e^2\rho\,, \qquad (6)$$

where ρ is the linear density of dissociable sites on DNA ($\rho = n/L$). These effects together explain the behavior of τ in figs. 7, where we find a satisfactory agreement between τ and τ_D.

$\Delta\epsilon$ and thus $\langle\mu^2\rangle$ decrease monotonically with increasing ethanol fraction, which is interpreted in terms of changes in $\langle S^2\rangle$ and α by eq. (4). Using the well-known relation $\eta_r \propto \langle S^2\rangle^{3/2}/M_r$ along with eqs. (3) and (4), we have

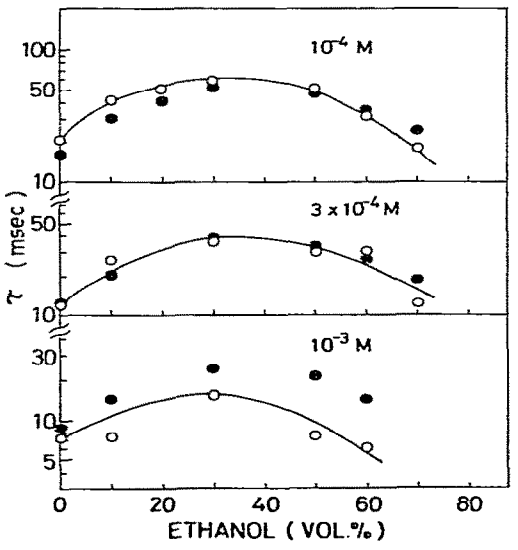

Fig. 7. Dielectric relaxation time (○) and rotational one (●) of DNA ($M_I = 2.5 \times 10^6$, $C_p = 0.1\,mg/cm^3$) in water ethanol mixtures at three NaCl concentrations (reproduced from Sakamoto, Hayakawa and Wada [14]).

$$\frac{\Delta\epsilon}{(\Delta\epsilon)_0} = \frac{\alpha(1-\alpha)}{\alpha_0(1-\alpha_0)}\left[\frac{\eta_r}{(\eta_r)_0}\right]^{2/3}, \qquad (7)$$

where the subscript 0 stands for an arbitrary reference state, zero ethanol concentration in this case. Equation (7) enables us to estimate α from observed values of $\Delta\epsilon$ and η_r. Values of α at each ethanol concentration were estimated from eq. (7) by taking $\alpha_0 = 0.3$. The α decreases gradually with increasing ethanol concentration and qualitatively agrees with α calculated by eq. (6).

3.5. Effect of salt binding

Cations in aqueous DNA shield the electrostatic repulsion between dissociated sites of DNA, resulting in the decrease of $\langle S^2 \rangle$ and furthermore, binding of cations on DNA affects α.

Fig. 8 draws $\Delta\epsilon$ and τ_D as functions of M/P (normality ratio of added cation to phosphate residue) at a constant DNA concentration for three kinds of salts. LiCl and tetramethylammonium chloride were found to have an effect similar to NaCl, and $CuCl_2$ and $MnCl_2$ were similar to $MgCl_2$. τ_D and $\Delta\epsilon$ decrease with increasing M/P for all salts but the effect is more enhanced for Ag^+ than other monovalent cations and is the strongest for divalent cations.

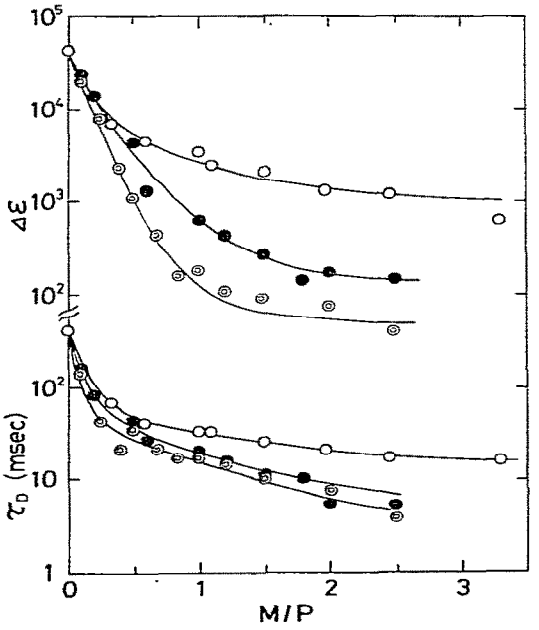

Fig. 8. $\Delta\epsilon$ and τ_D of aqueous DNA ($M_I = 4 \times 10^6$, $C_p = 0.01\%$) plotted against normality ratio of added salt and phosphate residue for three kinds of added salts: NaCl (○), $AgNO_3$ (●) and $MgCl_2$ (◎).

The rotational relaxation time τ calculated from reduced viscosity agree well with τ_D for all cation species and concentrations. The decrease in τ_D with increasing M/P is ascribed to the decrease in $\langle S^2 \rangle$ due to the shielding effect and also due to the decrease in α by ion binding.

$\Delta\epsilon$ in fig. 8 also decreases with increasing M/P owing to the decrease in both $\langle S^2 \rangle$ and α. By use of eq. (7) where we take $\alpha_0 = 0.3$ for $M/P = 2.5$ of NaCl as a reference, we get $\alpha = 0.05$ for $M/P = 2.5$ of Ag^+ and $\alpha = 0.01$ for $M/P = 2.5$ of divalent cations. These values reflect reasonably the binding affinity of these cations [27].

3.6. Effect of dye binding

It has been well documented that dye molecules such as acridine orange (AO) and methylene blue (MB) intercalate between base pairs of the double helix of DNA and with increasing dye concentration, the dye molecules are bound on the outside of the helix mainly

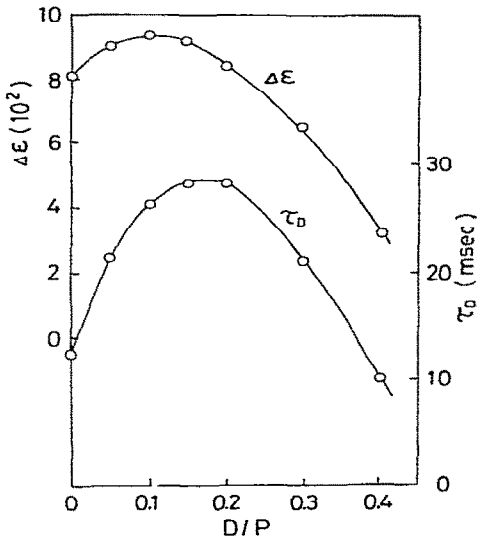

Fig. 9. $\Delta\epsilon$ and τ_D of aqueous DNA ($M_T = 2.5 \times 10^6$, $C_p = 0.01\%$, 0.3 mM NaCl) plotted against molarity ratio of acridine orange and phosphate residue.

by electrostatic attraction [28]. The intercalation is a very strong binding and is saturated at $D/P = 0.2$ (D/P being the molarity ratio of dye and phosphate residue) and then the external binding continues up to $D/P = 1$.

Fig. 9 shows $\Delta\epsilon$ and τ_D for DNA-AO systems plotted against D/P at a constant value of DNA concentration. τ_D has a maximum at $D/P = 0.18$ in fig. 9 and at $D/P = 0.11$ for DNA-MB systems. The reduced viscosity and τ calculated therefrom have the same dependence on D/P as τ_D and the ratio τ/τ_D is almost unity except high D/P of AO ($D/P > 0.6$) where the DNA-AO complex is formed. In the low D/P range, the intercalation lengthens the double helix and increases $\langle S^2 \rangle$ but at high D/P, the decrease of charge on DNA due to dye binding makes the molecule contract.

D/P dependence of $\Delta\epsilon$ has a maximum for AO (fig. 9) and a shoulder for MB. The behavior is interpreted in terms of changes in $\langle S^2 \rangle$ and α by eq. (4). By use of eq. (7) with a reference at $D/P = 0$, we can calculate α as a function of D/P. The α is almost equal to $\alpha_0 - (D/P)$ in the range of $D/P = 0$ to 0.2, being quite reasonable if we assume that, below $D/P = 0.2$, all dye molecules intercalate to DNA.

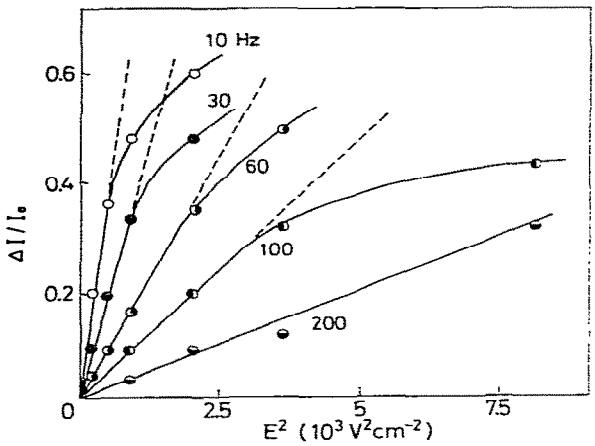

Fig. 10. Relative increment of scattered light intensity $r = \Delta I/I_0$ for aqueous DNA ($M_T = 5 \times 10^6$, $C_p = 0.05\%$, 0.1 mM NaCl) plotted against squared amplitude of electric field (reproduced from Fujikado, Hayakawa and Wada [16]).

3.7. Light scattering under a.c. electric field

When a prolate molecule with a permanent dipole μ along its major axis is oriented under an electric field, the scattered light intensity at a definite scattering angle θ increases (electric field light scattering) [29]. For a sinusoidally varying field with amplitude E and angular frequency ω, the relative change of scattered light intensity (steady component) is given by

$$r = C[(\mu/kT)^2/(1+\omega^2\tau^2) + \Delta\alpha/kT]E^2 + O(E^4), \quad (8)$$

where C is the constant depending on θ and shape and size of molecule relative to wavelength of light, τ the rotational relaxation time and $\Delta\alpha$ the anisotropy in electrical polarizability of the molecule.

As illustrated in fig. 10, the E^2 dependence of r for aqueous DNA was found to be linear up to a definite value of r. The deviation from the linearity starts at $E = 20$ V/cm for 10 Hz in fig. 10. Since this critical field at a sufficiently low frequency should correspond to $\mu E \simeq kT$, we can estimate as $\mu \simeq 0.6 \times 10^6$ D for this sample, which roughly agrees with the dipole moment obtained from the dielectric relaxation.

The dispersion curve for aqueous DNA of a lower molecular weight at $E = 72$ V/cm (linear range) and its FM curve are shown in fig. 11. The peak of the FM curve is located at 300 Hz, yielding $\tau = 0.53$ ms, which is comparable with the dielectric relaxation time of

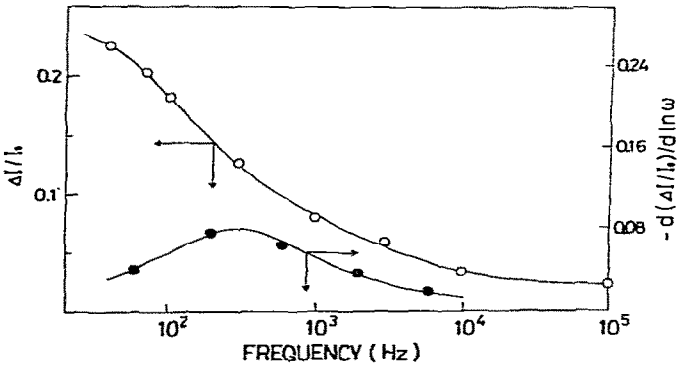

Fig. 11. Relative increment of scattered light intensity $r = \Delta I/I_0$ and its frequency derivative plotted against frequency of applied field (amplitude = 72 V/cm) for aqueous DNA ($M_I = 8.\times 10^5$, $C_p = 0.05\%$, 0.1 mM NaCl) (reproduced from Fujikado, Hayakawa and Wada [16]).

DNA of the same molecular weight, $\tau_D = 0.68$ ms (both reduced to 25°C).

The results of electric field light scattering clearly evidences that DNA possesses an elongated form and rotates under electric field. Dynamic electro-birefringence [17] and dynamic flow birefringence studies [18] on aqueous DNA recently carried out in our laboratory seem to support this conclusion.

Acknowledgements

This work was partly supported by a Grant-in-Aid for Scientific Research from the Ministry of Education of Japan. Permissions of John Wiley and Sons, Inc. for reproducing figures in their publications are gratefully acknowledged.

References

[1] S. Takashima, J. Mol. Biol. 7 (1963) 455.
[2] S. Takashima, J. Phys. Chem. 70 (1966) 1372.
[3] S. Takashima, Adv. Chem. Ser. 63 (1967) 232.
[4] S. Takashima, Biopolymers 5 (1967) 899.
[5] S. Takashima, Biopolymers 12 (1973) 145.
[6] D.N. Goswami and N.N. Das Gupta, Biopolymers 12 (1973) 1049.
[7] D.N. Goswami and N.N. Das Gupta, Biopolymers 13 (1974) 391.
[8] D.N. Goswami and N.N. Das Gupta, Biopolymers 13 (1974) 1549.
[9] M. Hanss and J.C. Bernengo, Biopolymers 12 (1973) 2151.
[10] M.S. Tung, R.J. Molinari, R.H. Cole and J.H. Gibbs, Biopolymers 16 (1977) 2653.
[11] Th. Vreugdenhil, Ph.D. Thesis (1977), State University of Leiden, The Netherlands.
[12] M. Sakamoto, H. Kanda, R. Hayakawa and Y. Wada, Biopolymers 15 (1976) 879.
[13] M. Sakamoto, R. Hayakawa and Y. Wada, Biopolymers 17 (1978) 1507.
[14] M. Sakamoto, R. Hayakawa and Y. Wada, Biopolymers 18 (1979) 2769.
[15] M. Sakamoto, R. Hayakawa and Y. Wada, Biopolymers (*in press*).
[16] T. Fujikado, R. Hayakawa and Y. Wads, Biopolymers 18 (1979) 2303.
[17] H. Aoyagi, Y. Mori, R. Hayakawa and Y. Wada, Repts. Progr. Polymer Phys. Japan 21 (1978) 625.
[18] N. Ookubo, T. Kiriki, K. Kuboyama, R. Hayakawa and Y. Wada, Repts. Progr. Polymer Phys. Japan 22 (1979) 687.
[19] H. Okamoto, H. Nakajima and Y. Wada, J. Polymer Sci. Polymer Phys. Ed. 12 (1974) 1035.
[20] S. Fujimori, M. Doi, H. Nakajima and Y. Wada, J. Polymer Sci. Polymer Phys. Ed. 13 (1975) 2135.
[21] R. Hayakawa, H. Kanda, M. Sakamoto and Y. Wada, Jpn. J. Appl. Phys. 14 (1975) 2039.
[22] S. Umemura, M. Sakamoto, R. Hayakawa and Y. Wada, Biopolymers 18 (1979) 25.
[23] H. Yamakawa, Modern theory of polymer solutions (Harper and Row, New York, 1971).
[24] F. Van der Touw and M. Mandel, Biophys. Chem. 2 (1974) 218.
[25] B.H. Zimm, J. Chem. Phys. 24 (1956) 269.
[26] G.S. Manning, J. Chem. Phys. 51 (1969) 924.
[27] I. Sissoëff, J. Grisvard and E. Guillé, Progr. Biophys. Mol. Biol. 31 (1976) 165.
[28] A. Blake and A.R. Peacocke, Biopolymers 6 (1968) 1225.
[29] B.R. Jennings, in: Molecular electro-optics, Part 1, ed. C.T. O'Konski (Marcel Dekker, New York, 1976) p. 275.